2013 IEEE/RSJ International Conference on
Intelligent Robots and Systems (IROS)
November 3-7, 2013. Tokyo, Japan

Identification of a Piecewise Controller of Lateral Human Standing Based on Returning Recursive-Least-Square Method

Nobuyuki Murai, Daishi Kaneta and Tomomichi Sugihara

Abstract— **This paper proposes an identification technique of a human standing controller. The dynamics of a human is approximated by the macroscopic relationship between the center of mass and the zero-moment point. The standing controller is modelled by a piecewise-linear feedback, which was originally developed for humanoid robots. In the previous work, the authors found a qualitative similarity of the model to an actual human behavior observed in a phase space, and the next challenge was to identify the controller from those data. A difficulty is that the observed dynamics is a piecewise system due to the unilaterality of reaction forces, so that the identification is not straightforward. It is not trivial how to detect the switching point in each motion locus and how to find the trust region of the supposed model. The recursive-least-square (RLS) method, which can present the deviation of identified parameters and that of the reliability of the results, helps to estimate the trust region with a returning computation process. Through the identification, the validity of the proposed method was verified. More study about the availability of the COM-ZMP model and the piecewise-linear controller for the analyses of the human standing control is also reported.**

I. Introduction

To understand motional properties of humans in a quantitative manner provides lots of knowledge not only in biological but also in engineering aspects. It is utilized to measure motion abilities and to model responsive characteristics of humans in medical diagnoses, athletic trainings, rehabilitations, ergonomic designs and so forth. The recent advancement of motion measurement technologies has enabled detailed modeling of human bodies[1] and even realtime monitoring of the internal activities of muscles and nerves[2]. However, no matter how precisely the human motion is computed, it doesn't necessarily suggest a clear explanation about the principle of motor control of humans. Although there have been many important studies related with the identification of human controllers, they basically targeted rather simple motions comprising only a couple of joints such as an arm-reaching[3], [4], [5] and a standing stabilization[6], [7], [8], [9]. The dynamical complexity of the human motion which is characterized by hyper-redundancy, underactuatedness and structure-varying property makes the problem challenging.

On the other hand, several techniques to control humanoid robots have been compiled in the field of robotics. It is known in particular that the macroscopic relationship between the center of mass (COM) and the center of pressure (COP), which is also named the zero-moment point (ZMP)[10], works for a hierarchical design of the whole-body controllers [11], [12], [13], [14], [15], [16], [17], [18], [19] for it captures the macroscopic dynamics of a humanoid.

Sugihara[19] proposed a piecewise-linear feedback controller for humanoid robots to stabilize COM during standing based on the above relationship between COM and ZMP, which we call the COM-ZMP model hereafter. In order to quantify a human's overall motion ability such as responsivity and equilibratory sense, it would be a better thought to focus on that macroscopic dynamics than to pay attention to each muscle, nerve or bone. In fact, Kaneta et al.[20], [21] observed a human's lateral COM movements in a phase space and found that the controller also matches the human's standing behavior qualitatively. It had been required to identify the controller from those data. A difficulty is that the observed dynamics is a piecewise system due to the unilaterality of reaction forces, so that the identification is not straightforward. It is not trivial how to detect the switching point in each motion locus and how to find the trust region of the supposed model of each segment.

The main objective of this paper is to propose an identification technique of a human standing controller utilizing the recursive-least-square (RLS) method[22]. It is originally for online parametric regressions and can present a history of the deviation of identified parameters and that of the reliability of the results. Those pieces of information help to estimate the trust region of the supposed model with a returning computation technique. The idea is that, when conducting RLS computation along with a motion locus, the deviation is reduced after going into the trust region, and by conducting RLS computation inversely from the end of the locus, the deviation increases after going out of the region so that we can obtain more reliable estimation of the trust region.

We conducted the identification and verified the validity of the proposed method, though it still has some problems to be improved. We also learned more about the availability of the COM-ZMP model and the piecewise-linear controller for the analyses of the human standing control.

II. Standing control scheme based on the COM-ZMP model

The dynamics of a humanoid, which could be either a real human or a humanoid robot, is represented by a complex equation of motion with a large dimensional generalized coordinates and inequality constraints originated from the limitation of reaction forces [23]. It is known, however, that the relationship between COM and ZMP well approximates

This work was supported by Grant-in-Aid for Young Scientists (A) #22680018, Japan Society for the Promotion of Science

N. Murai and T. Sugihara (zhidao@ieee.org) are with Department of Adaptive Machine Systems, Osaka University, Japan

D. Kaneta used to be with Department of Adaptive Machine Systems, Osaka University, Japan

978-1-4673-6357-0/13/$31.00 ©2013 IEEE

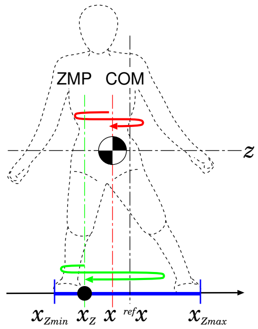

Fig. 1. The COM-ZMP model of a lateral standing motion

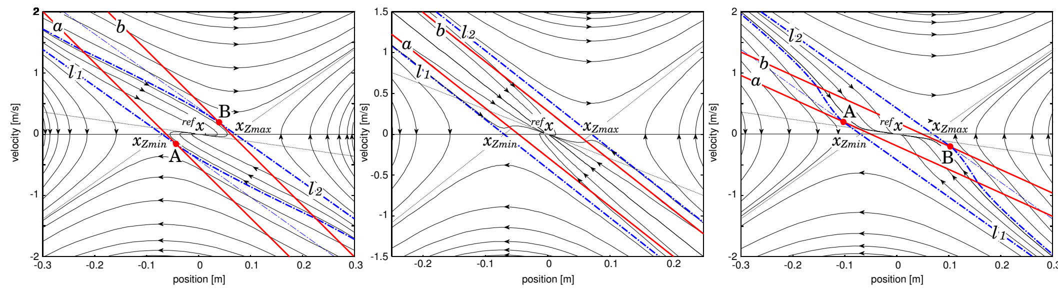

(a) $q_1 = 0.2, q_2 = 0.6$ (b) $q_1 = 0.5, q_2 = 1.0$ (c) $q_1 = 0.2, q_2 = 2.0$

Fig. 2. Phase portraits of the COM-ZMP model and the piecewise-linear controller with respect to different eigenvalues

the macroscopic characteristics of a humanoid through many studies on robot controls as referred in the introduction.

Let us consider a human motion in the lateral plane as shown in Fig. 1. Suppose the torque about COM is sufficiently smaller to be neglected than that due to the translational movement of COM about ZMP, we get the equation of motion as

$$\ddot{x} = \omega^2 (x - x_Z) \tag{1}$$

$$\omega \equiv \sqrt{\frac{\ddot{z} + g}{z}} \tag{2}$$

where x is the lateral position of COM, x_Z is the lateral position of ZMP, z is the height of COM with respect to the ground, and $g = 9.8$[m/s^2] is the acceleration due to the gravity. ZMP is constrained in the supporting region as

$$x_{Z\min} \le x_Z \le x_{Z\max}, \tag{3}$$

where $x_{Z\min}$ and $x_{Z\max}$ are the right and the left ends of the supporting region in x-axis, respectively. The above constraint comes from the unilaterality of reaction forces, namely, the fact that any attractive forces cannot act at any contact points.

Sugihara[19] proposed a controller in which the desired ZMP $^d x_Z$ is decided by a piecewise-linear feedback of COM state as

$$^d x_Z = \begin{cases} x_{Z\max} & (\text{S1:}\tilde{x}_Z \ge x_{Z\max}) \\ \tilde{x}_Z & (\text{S2:}x_{Z\min} < \tilde{x}_Z < x_{Z\max}) \\ x_{Z\min} & (\text{S3:}\tilde{x}_Z \le x_{Z\min}) \end{cases} \tag{4}$$

$$\tilde{x}_Z \equiv {}^d x + k_1 (x - {}^d x) + k_2 \dot{x}, \tag{5}$$

where $^d x$ is the referential position of COM and k_1 and k_2 are feedback gains. If the actual ZMP, which works as the input to the system, is manipulated to track the desired ZMP, the feedback system becomes

$$\ddot{x} = \begin{cases} \omega^2 x - \omega^2 x_{Z\max} & (\text{S1}) \\ -\omega^2 (k_1 - 1)(x - {}^d x) - \omega^2 k_2 \dot{x} & (\text{S2}) \\ \omega^2 x - \omega^2 x_{Z\min} & (\text{S3}) \end{cases}. \tag{6}$$

If we suppose that the COM height is invariant during the motion, namely, z is constant, ω is also constant and accordingly the system is piecewise-affine. In the case of

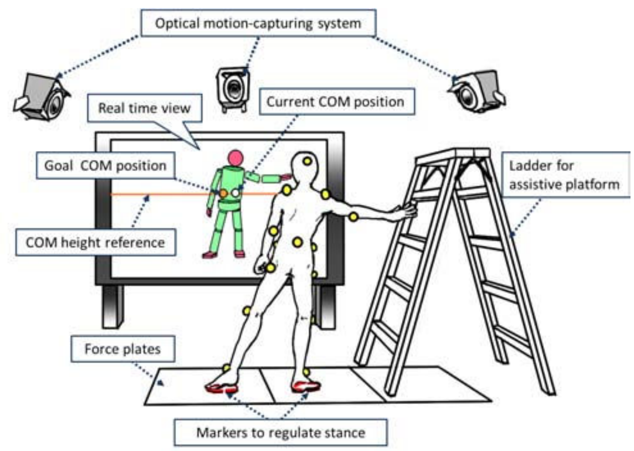

Fig. 3. Motion measurement system setup

robot control, the gains can be defined based on the pole assignment technique. Suppose the desired poles in (S2) are given as $-\omega q_1$ and $-\omega q_2$. Then, k_1 and k_2 are

$$k_1 = q_1 q_2 + 1, \quad k_2 = \frac{q_1 + q_2}{\omega}. \tag{7}$$

Fig. 2 shows phase portraits of the feedback system with respect to some different poles. The red lines a and b in the portraits mean the switching plane between (S1), (S2) and (S3); the region between a and b is (S2). (S1) and (S2) are separated by a, and (S2) and (S3) by b. The blue dotted areas are stable regions, where COM stably converges to the referential position.

Although this controller is simple with a small number of parameters for modelling the human behavior, it has the following virtues comparing to the previous standing models [6], [7], [8], [9].

1) It is almost free from body constitution of the subject, so that it suggests a macroscopic understanding of the whole-body behavior.
2) Effects of body constitution appears as perturbations, which is rather easily separated from the dominant behavior of the system, so that it suggests a hierarchical structure of the controller.
3) It explicitly deals with the dynamical constraint due to the unilaterality of reaction forces, which is hard when observing only behaviors of each joint.

(a) COM movement around the referential position

(c) over-accelerated movement, eventually falling down

(d) recovery movement from a point beyond the stance

(e) unrecovered movement outside of the stance

Fig. 4. Snapshots of experimental scenes

4) It enables quantitative evaluation of the controller. Stabilizability and responsivity are quantified by the system eigenvalues.

III. Visualization of the COM-ZMP dynamics

When considering to apply the model in the previous section to the identification of a human controller, a sufficient number of loci of COM in a phase space have to be collected. For this purpose, Kaneta et al.[20] conducted a motion measurement experiment. They found that the visualized loci qualitatively conform the phase portrait of the model, while they learned that the dispersion of convergence points and variation of the COM height during motions influence the reliability of data more than expected. Based on this, Kaneta et al.[21] redesigned the protocol and conducted another experiment in order to improve the accuracy of measurement by visually presenting the referential position and to see the effect of linear approximation in the model by controlling and uncontrolling the height of COM of the subject as illustrated in Fig. 3. This section summarizes it.

The subject was a 21-year-old male, who was 181[cm] tall and weighed 70[kg]. His kinematics and dynamics were modeled and identified before the experiments based on a method proposed by Ayusawa et al.[24]. The subject was informed the objective and risk of the experiment and understood them in advance. In the system, 3D loci of a set of the retroreflective markers attached to the subject's whole-body were measured every 5[ms] and were converted to a locus of the whole-body configuration through the inverse kinematics. The locus of COM was computed through the forward kinematics based on the subject's mass property. Measurement noises were reduced by a second-order Butterworth filter with 2[Hz] of cutoff frequency. By numerically differentiating it, a history of the velocity and acceleration of COM were computed. The locus of ZMP was also computed from a record of force plates. Fig. 4 shows snapshots of scenes of the experiment, where (a) is a recovery motion to the referential position against a perturbation, (c) is a falling-down motion over the point of equilibrium, (d) is a stabilization from a state in a distance of the point of equilibrium, and (e) is an unreaching motion from a state outside of the stable region to the point of equilibrium. 8 loci for the above 4 types of motions were collected in symmetric

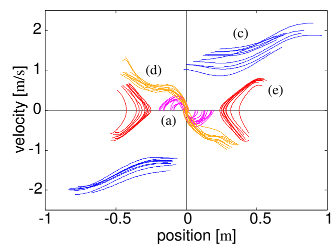

(A) COM height uncontrolled

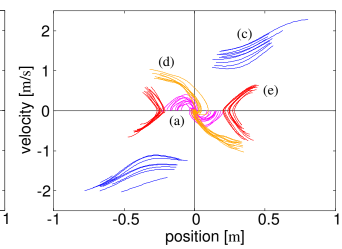

(B) COM height controlled

Fig. 5. Loci of COM of standing motions

manners with respect to the point of equilibrium under the condition with both uncontrolled and controlled COM height. Hence, the number of the loci was 128 in total. For the detail of the experiment, refer the original paper.

As the result, two sets of loci were obtained as Fig. 5(A) and (B), where the referential position is set to be the original point, namely, ${}^{d}x \equiv 0$. (A) is one with uncontrolled COM height, while (B) is with controlled COM height. Though the global structure of the measured behaviors in the two cases are similar, the difference of the condition qualitatively appears in the two figures; the loci of (A) in a distance of the point of equilibrium are distorted from the theoretic curves of the linear dynamics, while that of (B) are not.

Note that this study doesn't aim at making statistics to generalize the model but currently at presenting a method to identify an individual controller, so that the number of subjects doesn't concern.

IV. Identification of a piecewise-linear controller using RLS method with a returning process

Now, our objective is to identify the system parameters ω, $x_{Z\min}$ and $x_{Z\max}$ in Eqs.(1), (3), and the control parameters k_1 and k_2 in Eq.(5) from the result in the previous section, and have the following two problems to be solved:

1) Though ω is assumed to be constant in the model for simplicity, in fact, it varies during the motions particularly due to the limitation of leg length and accordingly the variation of COM height. How can the trust region of the model be bounded?
2) The control scheme might have been switched during a stable motion in accordance with Eq.(5). How can

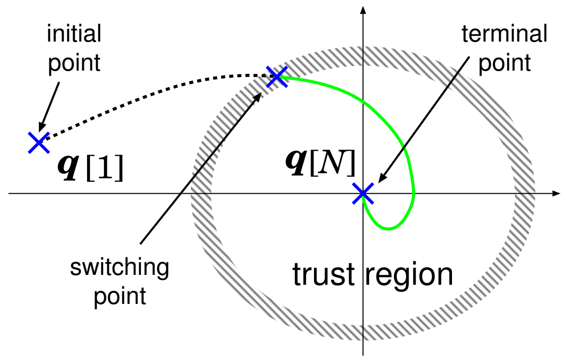

Fig. 6. A sampled locus and the trust region of the supposed model

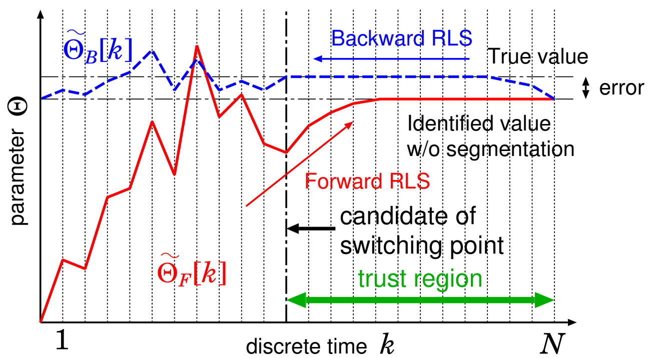

Fig. 7. RLS method with a returning process to estimate the trust region

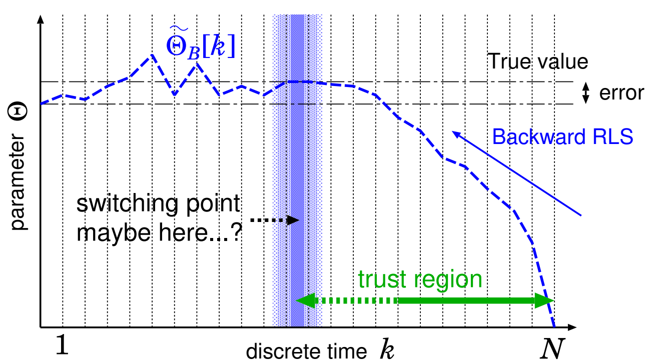

Fig. 8. If only conducting backward RLS, it is hard to find the boundary of the trust region

the switching point be detected?

Basically, the above problems have a common structure. Namely, both of them require the segmentation of data set based on the reliability of the supposed model and the parametric identification from the segmented data, which is one of the difficulties of the identification of piecewise systems.

Figs. 6 and 7 depicts our idea to solve this by utilizing the recursive-least-square (RLS) method[22] with a returning process. Suppose we have a locus of the state vector $\boldsymbol{q}(t)$, which is discretized with a sampling interval Δt into $\{\boldsymbol{q}[k]\}$ $(k = 1 \sim N)$, where $\boldsymbol{q}[k] \equiv \boldsymbol{q}(k\Delta t)$ and N is the number of samples. Let us consider a model of the system $\boldsymbol{\Theta}^{\mathrm{T}}\boldsymbol{q} = 0$ ($\boldsymbol{\Theta}$ is a set of parameters to be identified), which is valid only when $\boldsymbol{q} \in \mathcal{S}$, and a situation that the boundary of $\mathcal{S}$ is unknown. We have to detect the switching point at which the locus enters the trust region of $\mathcal{S}$, and identify $\boldsymbol{\Theta}$ only from the data within the trust region.

By applying the RLS method from $\boldsymbol{q}[1]$ to $\boldsymbol{q}[N]$ (forward RLS) under the model, the identified value of $\boldsymbol{\Theta}$, $\tilde{\boldsymbol{\Theta}}_F[k]$, is optimally updated at each step in the sense of the least square. Since the former part of the locus is not in $\mathcal{S}$ as illustrated in Fig. 6, the behavior of $\boldsymbol{q}[k]$ is inconsistent with the model and $\tilde{\boldsymbol{\Theta}}_F[k]$ unconverges. After the locus enters the trust region and matches the model, $\tilde{\boldsymbol{\Theta}}_F[k]$ is expected to converge gradually to a certain value as the red solid line in Fig. 7. The final value $\tilde{\boldsymbol{\Theta}}_F[N]$ would have an error from the true value of $\boldsymbol{\Theta}$ due to the influence of the model mismatch in the former part. Then, by applying the RLS method again but from $\boldsymbol{q}[N]$ to $\boldsymbol{q}[1]$ (backward RLS) with the initial guess $\tilde{\boldsymbol{\Theta}}_F[N]$, the identified value $\tilde{\boldsymbol{\Theta}}_B[k]$ is expected to converge to a certain value with better accuracy than the forward RLS as the blue dashed line in Fig. 7. After the locus goes out of the trust region, the behavior becomes inconsistent again with the model and $\tilde{\boldsymbol{\Theta}}_B[k]$ begins to fluctuate as well as the former part of $\tilde{\boldsymbol{\Theta}}_F[k]$. The final value $\tilde{\boldsymbol{\Theta}}_B[1]$ equals to $\tilde{\boldsymbol{\Theta}}_F[N]$ if the forward RLS starts with a sufficiently large covariance. Through this returning process, we can guess that the point from which $\tilde{\boldsymbol{\Theta}}_B[k]$ begins to stray is the switching point and the partial locus after this point is within the trust region.

Only the backward RLS might work if the convergence within the trust region is sufficiently rapid. We think that the above reciprocal process is preferable for more reliable estimation since in some cases the estimation doesn't converge to the true value within the trust region as Fig. 8 depicts.

In the case that a locus starts within $\mathcal{S}$ and goes out of it, the process in the reverse order is available, namely, one can conduct the backward RLS first and then the forward RLS.

V. Results and Discussion

A. Identification of the system parameters

The proposed idea is applicable to the identifications of both the system parameters and the control parameters. First, the identification of the system parameter ω was conducted in accordance with all the collected loci. 8 examples of the RLS computation with a returning process for each motion with uncontrolled and controlled COM height are shown in Fig. 9, where the red lines and the blue lines correspond to the lines of the same attribute in Fig. 7. Though they are no more than examples, the other also show similar profiles. As expected in the previous section, the estimated value of ω begins to converge to a certain value at a point in the forward RLS computation, while it begins to vary at another point in the backward RLS computation. Also as expected, the latter point in the backward RLS is earlier than the former point in the forward RLS in some cases, although those points don't differ much from each other in the other cases. It is contrary to the expectation, but the differences between the identified values in each computation are small. It means that the effect of model mismatch is not large at least on the sampled loci.

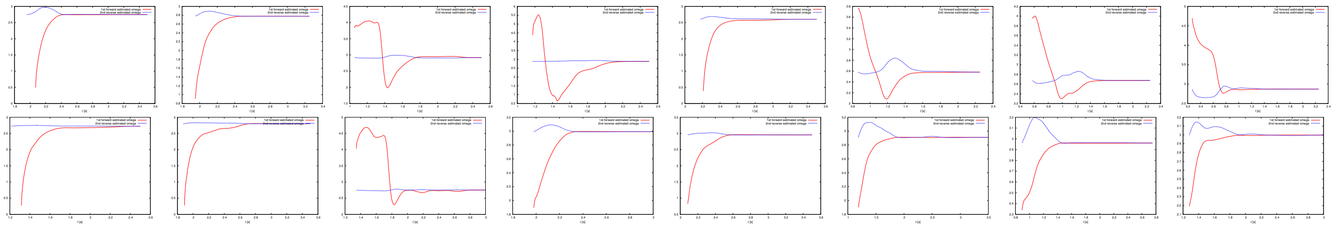

Fig. 9. History of the estimated ω corresponding to each locus with controlled COM height (top) and uncontrolled COM height (bottom) through returning RLS, red=forward RLS, blue: backward RLS

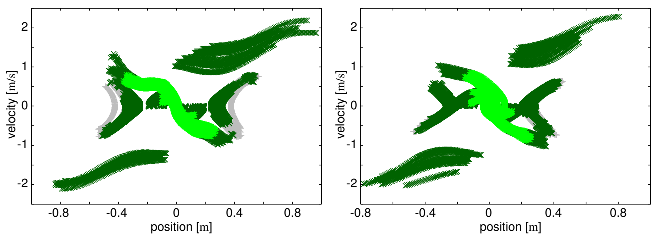

(A) COM height uncontrolled (B) COM height controlled

Fig. 10. Identified trust region of ω

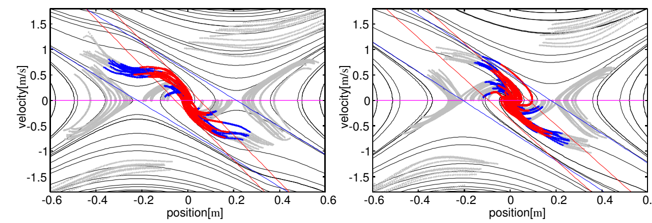

(A) COM height uncontrolled (B) COM height controlled

Fig. 12. Identified trust region of k_1 and k_2

Fig. 10 shows the resultant trust region with respect to ω. It was also unexpected, but the identified values were clustered to two groups in the both cases with uncontrolled and controlled COM height. In Fig. 10(A), which are the loci with uncontrolled COM height, the deep green lines mean those around $\omega \simeq 2.117$ while the light green lines mean those around $\omega \simeq 2.740$, where each value was identified through a batch least-square method of each clustered group. The reason why such clustering happened is easily imagined that the COM height is necessarily lowered in the distance of the point of equilibrium due to the limitation of leg length. In Fig. 10(B), which are the loci with controlled COM height, the deep green lines mean those around $\omega \simeq 2.808$ while the light green lines mean those around $\omega \simeq 2.914$, where each value was identified by the same method. Obviously, the difference between those two values is smaller than that of the case with uncontrolled COM height.

In the above procedures, the boundaries of the trust region were detected manually with respect to each locus. The identified values for each locus are not directly associated with the value computed throught the batch identification.

B. Identification of the control parameters

Next, the identification of the control parameter k_1 and k_2 was conducted as well. In this case, only the loci which stably converge to the referential position are available. Moreover, since the identified ω converged to two values, only the partial loci with a larger ω, namely, $\omega = 2.740$ for the cases with uncontrolled COM height and $\omega = 2.914$ for the cases with controlled COM height, were used.

Fig. 11 are examples of the RLS computation with a returning process, where the red line and the blue line correspond to the lines of the same attribute in Fig. 7. As well as the cases of the estimation of ω, the forward RLS and the backward RLS show similar profiles to that expected, and the boundaries of the trust region were manually detected with respect to each locus. Fig. 12 shows the resultant trust region with respect to k_1 and k_2, where $x_{Z\min}$ and $x_{Z\max}$, which are necessary to draw the blue asymptotic lines, were estimated from the record of the reaction force plates. The identified values are $(k_1, k_2) = (4.038, 0.875)$ for the cases with uncontrolled COM height, and $(k_1, k_2) = (2.204, 0.549)$ for the cases with controlled COM height. In the figures, the red part of the loci are evaluated to be within the trust region of (S2), while the blue part are within that of (S1) and (S3). Since (S2) are depicted as the region between the red lines, which are defined by ω, k_1 and k_2, one can see that the result shows a good estimation in the case with uncontrolled COM height (Fig. 12(A)). On the other hand, it is not clear whether the estimation is successful in the case with controlled COM height (Fig. 12(B)), since almost all the loci to which the proposed method was applied are evaluated to be within (S2). It was possibly because the trust region with respect to the identified ω is too conservatively estimated.

VI. Conclusion

An identification technique of a piecewise system utilizing RLS method was proposed and applied to a human standing controller. As the result, we have the following conclusions.

1) The availability of the COM-ZMP model and the piecewise-linear feedback controller was quantitatively assessed, though they still have some problems to be improved in terms of accuracy.
2) Though the assumption that the COM height is constant is violated in a distance of the point of equilibrium, the trust region of the linearlized COM-ZMP model under that assumption has a fair area.
3) The proposed technique works to find the trust region and the switching points of both the system parameters and the control parameters on each motion locus. The

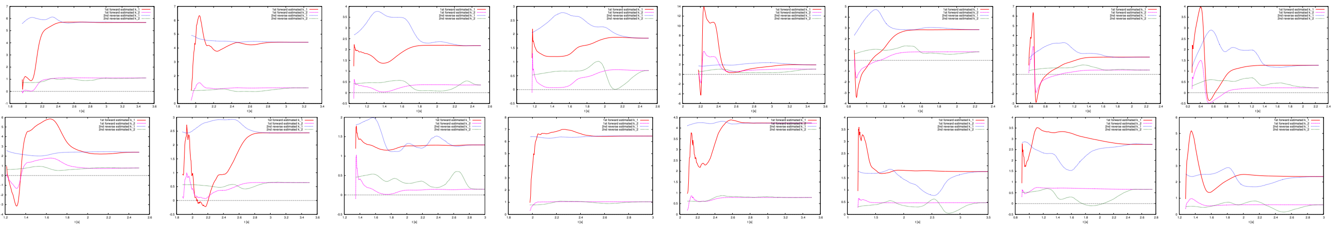

Fig. 11. History of the estimated k_1 and k_2 corresponding to each locus with controlled COM height (top) and uncontrolled COM height (bottom) through returning RLS, red&magenta=forward RLS, blue&green: backward RLS

authors had a good estimation of the trust region of the piecewise-linear controller in one case. In another case, however, the estimation was not very convincing. The estimation accuracy of the system parameter affected it.

4) Presently, the switching points are manually detected based on the history of the recursive estimation. They should be found numerically based on the reliability of the model. From this viewpoint, we might have to focus on the change of covariance. Other techniques for the identification of piecewise-affine systems[25], [26], [27] should also be examined.

ACKNOWLEDGMENT

The authors cordially express our gratitude to Prof. Yoshihiko Nakamura, Dr. Ko Ayusawa, Dr. Akihiko Murai, Mr. Yosuke Ikegami and other members of Nakamura-Takano laboratory in the University of Tokyo for their cooperation on the experiments.

REFERENCES

[1] A. Murai, K. Yamane, and Y. Nakamura, "Modeling and identification of human neuromusculoskeletal network based on biomechanical property of muscle," in *Proceedings of the 30th Annual International Conference of IEEE Engineering in Medicine and Biology Society*, 2008, pp. 3706–3709.

[2] A. Murai, K. Kurosaki, K. Yamane, and Y. Nakamura, "Musculoskeletal-see-through mirror: computational modeling and algorithm for whole-body muscle activity visualization in real time," *Progress in Biophysics and Molecular Biology*, vol. 103, no. 2-3, pp. 310–317, 2010.

[3] N. Hogan, "Impedance Control: An Approach to Manipulation," *Transaction of the ASME, Journal of Dynamic Systems, Measurement, and Control*, vol. 107, no. 1, pp. 1–24, 1985.

[4] T. Flash and N. Hogan, "The coordination of arm movements: an experimentally confirmed mathematical model," *The journal of Neuroscience*, vol. 5, no. 7, pp. 1688–1703, 1985.

[5] Y. Uno, M. Kawato, and R. Suzuki, "Formation and control of optimal trajectory in human multijoint arm movement," *Biological cybernetics*, vol. 61, no. 2, pp. 89–101, 1989.

[6] L. M. Nashner and G. McCollum, "The organization of human postural movements: a formal basis and experimental synthesis," *Behavioral and Brain Sciences*, vol. 8, no. 1, pp. 135–150, 1985.

[7] M. J. Mueller, D. R. Sinacore, S. Hoogstrate, and L. Daly, "Hip and ankle walking strategies: effect on peak plantar pressures and implications for neuropathic ulceration," *Archives of physical medicine and rehabilitation*, vol. 75, no. 11, p. 1196, 1994.

[8] P. Gatev, S. Thomas, T. Kepple, and M. Hallett, "Feedforward ankle strategy of balance during quiet stance in adults," *The Journal of physiology*, vol. 514, no. 3, pp. 915–928, 1999.

[9] A. H. Vette, K. Masani, and M. R. Popovic, "Implementation of a physiologically identified PD feedback controller for regulating the active ankle torque during quiet stance," *Neural Systems and Rehabilitation Engineering*, vol. 15, no. 2, pp. 235–243, 2007.

[10] M. Vukobratović and J. Stepanenko, "On the Stability of Anthropomorphic Systems," *Mathematical Biosciences*, vol. 15, no. 1, pp. 1–37, 1972.

[11] F. Miyazaki and S. Arimoto, "A Control Theoretic Study on Dynamical Biped Locomotion," *Transaction of the ASME, Journal of Dynamic Systems, Measurement, and Control*, vol. 102, pp. 233–239, 1980.

[12] J. Furusho and M. Masubuchi, "Control of a Dynamical Biped Locomotion System for Steady Walking," *Transactions of the ASME, Journal of Dynamic Systems, Measurement, and Control*, vol. 108, pp. 111–118, 1986.

[13] S. Kajita, T. Yamaura, and A. Kobayashi, "Dynamic Walking Control of a Biped Robot Along a Potential Energy Conserving Orbit," *IEEE Transactions on Robotics and Automation*, vol. 8, no. 4, pp. 431–438, 1992.

[14] K. Hirai, M. Hirose, Y. Haikawa, and T. Takenaka, "The Development of Honda Humanoid Robot," in *Proceeding of the 1998 IEEE International Conference on Robotics & Automation*, 1998, pp. 1321–1326.

[15] K. Mitobe, G. Capi, and Y. Nasu, "Control of walking robots based on manipulation of the zero moment point," *Robotica*, vol. 18, pp. 651–657, 2000.

[16] T. Sugihara, Y. Nakamura, and H. Inoue, "Realtime Humanoid Motion Generation through ZMP Manipulation based on Inverted Pendulum Control," in *Proceedings of the 2002 IEEE International Conference on Robotics & Automation*, 2002, pp. 1404–1409.

[17] J. Morimoto, G. Endo, J. Nakanishi, and G. Cheng, "A Biologically Inspired Biped Locomotion Strategy for Humanoid Robots: Modulation of Sinusoidal Patterns by a Coupled Oscillator Model," *IEEE Transactions on Robotics*, vol. 24, no. 1, pp. 185–191, 2008.

[18] S.-H. Hyon, "Compliant terrain adaptation for biped humanoids without measuring ground surface and contact forces," *IEEE Transactions on Robotics*, vol. 25, no. 1, pp. 171–178, 2009.

[19] T. Sugihara, "Standing Stabilizability and Stepping Maneuver in Planar Bipedalism based on the Best COM-ZMP Regulator," in *Proceedings of the 2009 IEEE International Conference on Robotics & Automation*, 2009, pp. 1966–1971.

[20] D. Kaneta, N. Murai, and T. Sugihara, "Visualization and Identification of Macroscopic Dynamics of a Human Motor Control Based on the Motion Measurement," in *Proceedings of the 2012 IEEE-RAS International Conference on Humanoid Robots*, 2012, pp. 767–772.

[21] ——, "Reassessment of COM-ZMP Model for the Identification of Lateral Standing Controller of a Human (to appear)," in *Proceedings of the 2013 IEEE/RSJ International Conference on Intelligent Robots and Systems*, 2013, pp. –.

[22] M. H. Hayes, *Statistical Digital Signal Processing and Modeling*. Wiley, 1996.

[23] Y. Fujimoto and A. Kawamura, "Simulation of an Autonomous Biped Walking Robot Including Environmental Force Interaction," *IEEE Robotics & Automation Magazine*, vol. 5, no. 2, pp. 33–41, 1998.

[24] K. Ayusawa, G. Venture, and Y. Nakamura, "Real-time implementation of physically consistent identification of human body segments," in *Proceedings of 2011 IEEE International Conference on Robotics and Automation*, 2011, pp. 6282–6287.

[25] G. Ferrari-Trecate, M. Muselli, D. Liberati, and M. Morari, "A clustering technique for the identification of piecewise affine systems," *Automatica*, vol. 39, no. 2, pp. 205–217, 2003.

[26] A. Bemporad, A. Garulli, S. Paoletti, and A. Vicino, "Set membership identification of piecewise affine models," in *Proceedings of 13th IFAC Symposium on System Identification*, 2003, pp. 1826–1831.

[27] R. Vidal, S. Soatto, Y. Ma, and S. Sastry, "An algebraic geometric approach to the identification of a class of linear hybrid systems," in *Proceedings of 42nd IEEE Conference on Decision and Control*, 2003, pp. 167–172.